Melting of Wigner electron crystals; phenomenology and anyon magnetism

1992 J. Phys.: Condens. Matter 4 5263

(http://iopscience.iop.org/0953-8984/4/23/003)

J. Phys.: Condens. Matter 4 (1992) 5263–5272. Printed in the UK

Melting of Wigner electron crystals: phenomenology and anyon magnetism

M J Lea†, N H March‡ and W Sung§

† Royal Holloway and Bedford New College, University of London, Egham, Surrey TW20 0EX, UK

‡ Theoretical Chemistry Department, University of Oxford, 5 South Parks Road, Oxford OX1 3UB, UK

§ Department of Physics, Pohang Institute of Technology, Korea

Received 19 December 1991

Abstract. The appropriate generalization of the Clausius–Clapeyron equation to describe the first-order melting transition of two-dimensional Wigner electron crystals is used (a) within a phenomenological framework and (b) in conjunction with microscopic theories relating to anyons and composite fermions, to represent the main features of the melting curve as a function of Landau level filling factor ν.

1. Introduction

The proposal of Durkan *et al* (1968) that Wigner electron crystallization should be aided by an applied magnetic field H has now been brought to fruition, starting with the experiment of Andrei *et al* (1988) on two-dimensional GaAs/AlGaAs heterojunctions. This work, in which preliminary data on the melting curve of the Wigner crystal in two dimensions as a function of field were presented, has subsequently been confirmed and extended (see Glattli *et al* 1991). Structure in the phase diagram was reported by Glattli *et al* (1991), Plaut *et al* (1991) and Li *et al* (1991). In particular Buhmann *et al* (1991), using luminescence measurements on the same system as that studied by Andrei *et al* (1988) have suggested a schematic phase diagram, giving the melting temperature T_m versus the Landau level filling factor $\nu = nhc/eH$, where n is the electron density, as shown in figure 1(*a*). The most notable features of this phase diagram are the re-entrant liquid phases. The latter work prompted us to give the thermodynamics of the Wigner crystal melting curve in a magnetic field H (Lea *et al* 1991). The main result of that study was for the slope of the melting curve in the (H, T_m) plane:

$$\partial T_m/\partial H = -\Delta M/\Delta S \tag{1}$$

where ΔM and ΔS represent the changes across the melting curve of the magnetization M and the entropy S respectively. The re-entrant aspects of the phase diagram plotted by Buhmann *et al* (1991) having maxima in the (H, T_m) plane, define points where $\Delta M = 0$. Rewriting (1) in terms of ν readily yields

$$\partial T_m/\partial \nu = (H/\nu)\,\Delta M/\Delta S. \tag{2}$$

0953-8984/92/235263+10$04.50

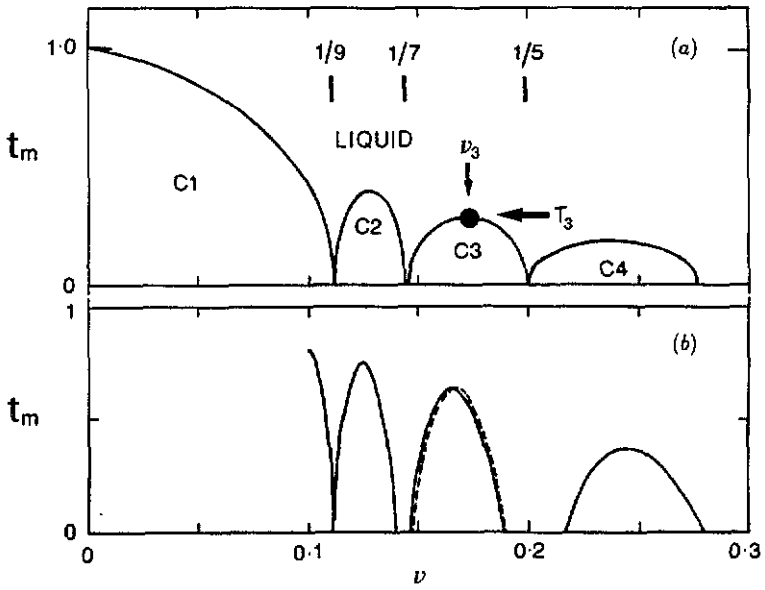

Figure 1. (*a*) Schematic phase diagram showing Wigner crystals in regions C_1–C_4 as proposed by Buhmann *et al* (1991). (*b*) Model calculations of the phase diagram. The solid lines show a model based on (10), (12) and (13) as described in the text. The dashed line in phase C3 only shows the schematic form given by the phenomenological equation (4).

It is clear from (2) that, to model the Wigner crystal melting curve, one must study the changes in magnetization ΔM, and the entropy ΔS.

The purpose of the present paper is twofold:

(i) to provide a phenomenological model that will allow the integration of (2);

(ii) to study the magnetism of the anyon model in the present context, bearing in mind the remarkable variation of the magnetism of the (Laughlin) electron liquid as a function of ν, deduced in our earlier work (Lea *et al* 1991). This also leads to an analysis based on composite fermions.

2. Phenomenological model

It seems natural enough, in view of the zeros in ΔM already referred to, at temperature T_3 and $\nu = \nu_3$, say, in region C_3 (see figure 1(*a*)), to express ΔM as an expansion in $\nu^{-1} - \nu_3^{-1}$. Assuming that the entropy difference along the melting curve is a maximum near ν_3 and falls to zero as T_m goes to zero, we can write (2) as

$$\partial T_m/\partial \nu \propto (H/\nu)(\nu^{-1} - \nu_3^{-1})/[1 - a(\nu^{-1} - \nu_3^{-1})^2] \tag{3}$$

where a is a constant close to unity, which can be integrated to give

$$T_m(\nu) = T_3[1 + C \ln(1 - a(\nu^{-1} - \nu_3^{-1})^2)] \tag{4}$$

where the parameters C and a must be determined experimentally. The form of $T_m(\nu)$ given by (4) is shown in figure 1(*b*), for the C_3 phase. Further terms in the expansion in $\nu^{-1} - \nu_3^{-1}$ could be included that would change the detailed shape of the phase boundaries. This analysis should apply between any two re-entrant phases.

3. Anyon model: classical limit

Having established a primitive phenomenological form appropriate to represent regions C_2–C_4 in figure 1, let us now turn to a model which can give further insight into the microscopic origin of the phase diagram. This is the anyon model, in which one has fractional statistics (Wilczek 1990) characterized by a parameter γ, which has the value 0 for fermions and the value $\pm\frac{1}{2}$ for bosons.

A dilute (non-degenerate) gas of non-interacting two-dimensional anyons (mass m) in a magnetic field has been studied by Johnson and Canright (1990) and also by Dowker and Chang (1990). The second virial coefficient B_2 in the equation of state for the pressure P,

$$P/nkT = 1 + nB_2(T) + O(n^2) \tag{5}$$

is given by

$$B_2(T) = (\lambda^2/x)[\gamma - \exp(4\gamma x)/(2\sinh(2x)) + 1/(4\tanh(x))] \tag{6}$$

where λ is the de Broglie thermal wavelength given by $\lambda^2 = h^2/2\pi mkT$, $x = \hbar\omega_c/2kT$ and ω_c is the cyclotron frequency. Hence the differential magnetization per unit area of the anyons relative to a classical gas is

$$\Delta M_a(\gamma) = -(n^2/2m)\,\partial B_2/\partial x. \tag{7}$$

This is shown in figure 2 as a function of γ for $x = 1$, 2, 5 and 10. Note that the magnetization is not symmetric about $\gamma = 0$, but does have the same value for $\gamma = \pm\frac{1}{2}$.

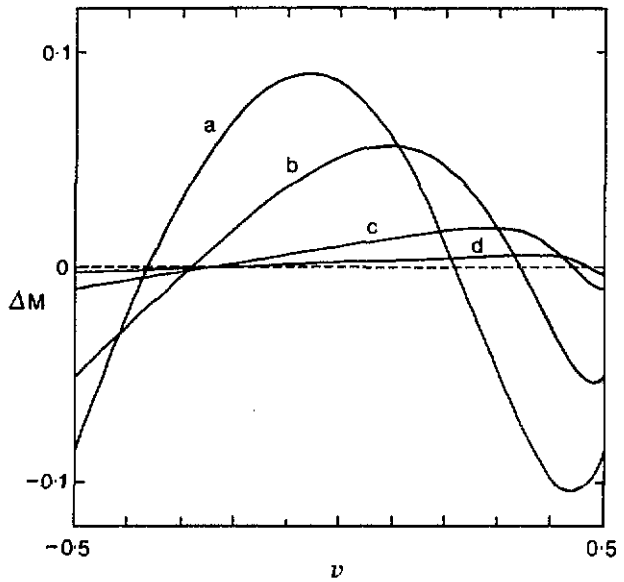

Figure 2. Anyon magnetism ΔM_a of an anyon gas according to (7), versus the fractional statistics parameter γ. Different curves (a–d) correspond to values of the parameter $x = 1$, 2, 5 and 10 respectively.

In order to relate (2) to a field-dependent magnetization it is necessary to relate the statistics parameter γ to ν. To gain orientation, let us refer back to figure 1. Taking the admittedly schematic form there literally, one notes that $T_m = 0$ at values $\nu = 1/q$, where $q = 9$, 7 and 5. At these very points, microscopic theory predicts a Bose condensate (Lee 1991), although this is immediately unstable against raising the temperature. However, this motivates the assumption that at $\nu = 1/q$ the value of γ corresponds to the boson value. Hence as the number of flux quanta per electron, $1/\nu$, increases, the particles alternate between fermions and bosons. Turning to the maxima in the melting curve in the (ν, T_m) plane, one has $\Delta M = 0$, and since the Wigner electron crystal is built from fermions, we expect that the first-order melting transition described by the analogue, equation (1), of the Clausius–Clapeyron equation will degenerate at these points to a second-order transition, since $\Delta M = 0$ there. Hence one assumes that the anyons are fermions at the maxima in the melting curve. The assumption that γ is a continuous variable between these limits is related to a mean-field approximation (Johnson and Canright 1990). If we assume that for non-integral values of q the particles are anyons with fractional statistics, then the magnetization will be dependent on the field, from (2).

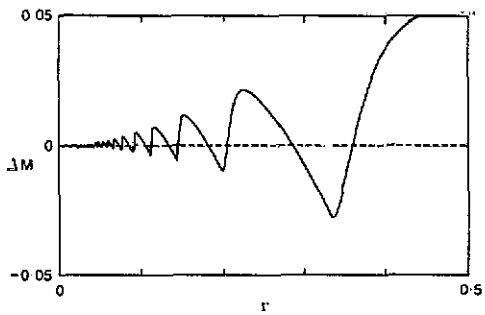

Figure 3. ΔM_a as a function of Landau level filling factor ν. This plot is obtained from figure 2 by using the γ–ν relation given in (8).

These ideas can be subsumed in the relation

$$\gamma = 1/2\nu - j \tag{8}$$

where the integer j is chosen in such a way that γ varies in the range from $-\frac{1}{2}$ to $+\frac{1}{2}$ as ν decreases. This assumption allows plots of the field-dependent ΔM_a versus ν of an anyon gas for various parameter values, from (5) and (6), as shown in figure 3. The plot is calculated for $x = A/\nu$, which corresponds to a variable field at a fixed temperature, for the arbitrary value $A = 1$. It can be seen that the magnetization of this non-interacting anyon gas has many of the features required to explain qualitatively the phase diagram of the 2D Wigner crystal. In particular, ΔM_a changes sign at $\nu = 1/q$ as required to explain the re-entrant nature of the solid regions C_2, C_3 and C_4. It also predicts that there may be further structure in the phase diagram of the region C_1, at $\nu = 1/q$, where q is an odd integer. It appears likely that the purely statistical effects described here will persist in the presence of interactions and that similar magnetization changes will also occur at the FQHE states, at integral fractions.

While, in view of the simplified nature of the assumption†, equation (7), we do not feel it appropriate to press the detail quantitatively, it seems remarkable that the anyon model does indeed extend the de-Haas–van-Alphen-type singularities referred to by Lea *et al* (1991) into the region $\nu \ll 1$.

4. Low-temperature treatment: composite fermion model

A closely related approach at low temperatures, in contrast to the classical limit discussed above, is to use the idea of 'composite' fermions (Jain 1989, 1990, 1992, Jain and Goldman 1992) in which a fermion plus an even number of flux quanta is also a fermion. These composite fermions are then regarded as separate entities in the magnetic field of the remaining flux lines, with a new filling factor ν_i given by

$$\nu_i = \nu/(1 - 2i\nu) = p/(q - 2ip) \tag{9}$$

where $2i$ is the number of flux quanta associated with each composite fermion. The second part of (9) gives ν_i for the fractional quantum Hall states with $\nu = p/q$. For each of these states a value of i can be chosen such that ν_i is an integer. The sign of ν_i depends on whether the flux in the composite fermion is parallel or anti-parallel to the applied field. For the FQHE states with $p = 1$, $\nu_i = 1$ with $i = 1, 2, 3, 4, 5$ for $q = 3, 5, 7, 9, 11$ and so on. This idea has been successfully used by Jain and Goldman (1992) to map the fractional quantum Hall effect states to equivalent integer quantum Hall effect states.

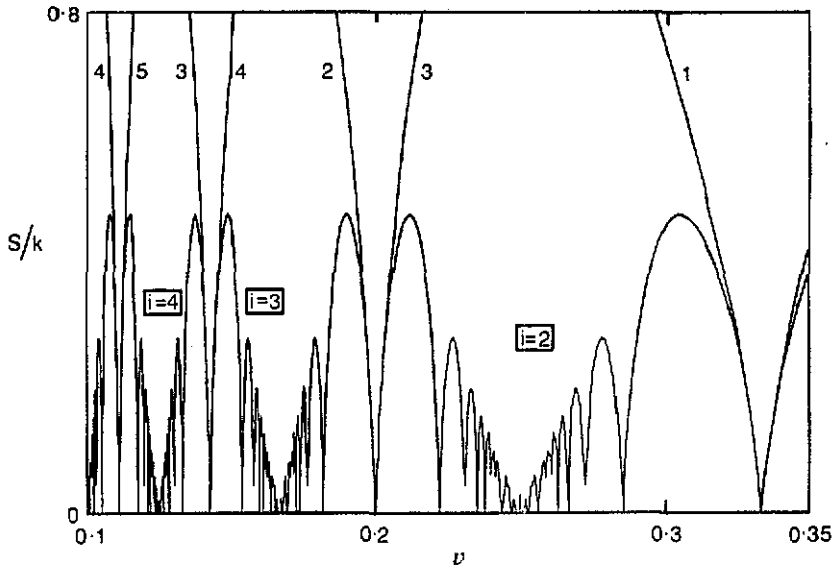

Figure 4. The entropy $S(\nu)/k$ per electron for the composite fermion model, calculated using (9). The various lines are marked by the value of i, the number of flux quanta pairs in each composite fermion. Note that $S(\nu)$ goes to zero at each ordered state $\nu = p/q$ of the fractional quantum Hall effect.

† We reiterate that the virial expansion used is only strictly valid in the classical limit.

4.1. Entropy of the composite fermions

If the entropy $S(\nu)$ of the liquid goes to zero at the fractional filling factors, then we can relate the entropy to the equivalent integer state based on ν_i. Using the results for the de Haas–van Alphen effect we have the entropy per electron $S(\nu)$ for a partially full level:

$$S(\nu) = (-k/\nu_i)[\nu_i \ln \nu_i + (1-\nu_i)\ln(1-\nu_i)] \tag{10}$$

for $\nu_i \leqslant 1$, and equivalent forms for $\nu_i > 1$, where ν_i is given by (9). The entropy of these fermions for $i = 1$, 2 and 3 is shown in figure 5 for $0.1 < \nu < 0.35$ and goes to zero at each ordered state of the fractional quantum Hall effect. This entropy expression will only be valid as long as the system behaves as an assembly of weakly interacting composite fermions. Note, however, that the entropy close to the $\nu = \frac{1}{5}$ state, for instance, has the same form for $i = 2$ and $i = 3$. The functional form of $S(\nu)$ between two neighbouring states is close to the phenomenological expression used in section 2. According to the third law of thermodynamics, the entropy $S(\nu)$ away from the ordered states must also go to zero in the very-low-temperature limit. This could occur via further ordering among the excitations or, in real systems, via some form of localization due to random potentials, as in the integer quantum Hall effect, which could also lead to the observed Hall plateaus. The effect of these localizing potentials would presumably also lead to a pinned Wigner crystal as the solid ground state, as also observed experimentally (Glattli *et al* 1991).

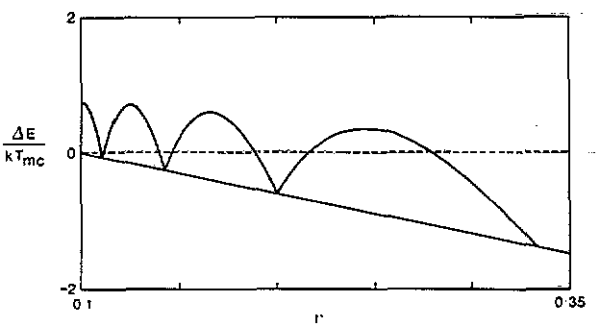

Figure 5. Form of internal energy along the melting curve, expressed as $\Delta E/kT_{mc}$. Gradients at the displayed cusps in ΔE are known in terms of excitation energies and the energy gaps Δ_ν. This information is used asymptotically in this figure at $\nu = 1/q$. The turning points shown in ΔE versus ν are as required by the thermodynamic arguments presented by Lea *et al* (1991).

4.2. Energy of the electron liquid

The internal energies (including the magnetic potential energy term $-HM$, which is different from the definition employed by Lea *et al* (1991) of the electron liquid and solid have been calculated by several authors (see Isihara (1989) for a review). For $\nu \leqslant 0.1$ the solid is thought to have the lower free energy at $T = 0$ and is then the ground state. The Laughlin liquid states have the lower ground-state energies for $\nu = 1/q$ where $q = 3,5,7$ and probably 9. If the temperature T of one of these states is increased, then quasi-particle excitations are thermally excited across an energy gap

Δ. Tao (1990) has shown that this energy gap is field dependent and must have the form

$$\Delta = \Delta_\nu e^2/l \qquad \Delta/kT_{mc} = \Gamma_m \Delta_\nu \sqrt{2/\nu} \tag{11}$$

where $l = (\hbar c/eH)^{1/2}$ is the magnetic length, and Δ_ν is a dimensionless parameter to be calculated or found from experiment. For $\nu = 1/q = \frac{1}{3}$, $\Delta_\nu = 0.018$ (Isihara 1989). The second part of the equation gives the energy gap in units of the transition temperature of the classical electron gas $T_{mc} = e^2(\pi n)^{1/2}/k\Gamma_m$ where $\Gamma_m = 127$ (Deville 1988). If the magnetic field is increased or decreased then quasi-particle or quasi-hole excitations will be generated with energies ϵ_+ and ϵ_- respectively where $\epsilon_+ + \epsilon_- = \Delta$, since an increase in temperature creates neutral pairs of excitations. If an excitation is equivalent to an extra or missing flux line then we can write the energy per electron near $\nu = \nu_q = 1/q$ as

$$E(\nu) = E_q + [|(\nu - \nu_q)|/\nu_q]q\epsilon_\pm \tag{12}$$

where E_q is the ground-state energy at $\nu = 1/q$. Hence the energy $E(\nu)$ will have cusps at $\nu = 1/q$, as shown in figure 5.

4.3. Magnetization of the electron liquid

The magnetization $M = -(\partial F/\partial H)_T$ where F is the free energy $F = E - TS$. At zero temperature, a cusp in the energy near ν_q, for instance, will give a jump in the magnetization per electron of magnitude $q(\epsilon_+ + \epsilon_-)/H = q\Delta/H$ as ν passes through the ordered state. Hence the magnetization may change sign as ν passes through each of the ordered states indicated by $S = 0$ in figure 5. The schematic variation of M with ν will therefore be very similar in structure to the diagram for the anyon gas in figure 3, although many more states may be revealed.

4.4. The liquid–solid phase diagram

We can now return to the discussion of the field dependence of the electron–solid phase boundary. If the liquid phases at $\nu \simeq \frac{1}{3}, \frac{1}{5}, \frac{1}{7}$ and $\frac{1}{9}$ do have lower internal energy than the solid they will form the ground state at zero temperature. For $\nu < \nu_q$ the energy will increase as excitations are created until $E_S = E_L$ (the subscripts refer to the solid and liquid phases). At this point there will be a phase transition to the solid phase. Hence the phase diagram will indeed contain re-entrant liquid phases as proposed by Buhmann *et al* (1991). The experimental evidence indicates that these occur at $\nu = \frac{1}{5}, \frac{1}{7}$ and $\frac{1}{9}$ while Plaut *et al* (1991) found that the highest value of ν for which the solid was present was $\nu = 0.28 \pm 0.02$. However, it must be noted that in the original results of Andrei *et al* (1988) a possible solid phase was found for $\nu \simeq 0.34$. Glattli *et al* (1991) have also reported a liquid phase close to $\nu = \frac{2}{9}$ which would correspond to $i = 2$, $\nu_i = 1$ in (9). We can use the experimental value of Plaut *et al* (1991) to determine $\Delta E = E_L - E_S$ at $\nu = \frac{1}{3}$ by assuming $\epsilon_+ = \epsilon_- = \Delta/2$ with $\Delta_\nu = 0.009$ (Isihara 1989) in (12), so that $\Delta E = 0$ at $\nu = 0.28$. If we also assume that ΔE at the ground states $\nu = \nu_q$ decreases in magnitude until the solid phase becomes the only stable phase for $\nu > 0.1$ (see Isihara 1989), we can then sketch $\Delta E(\nu)$ along the melting curve, expressed in units of kT_{mc} as shown in figure 6. The gradients at the cusps in ΔE are determined by the excitation energies and the

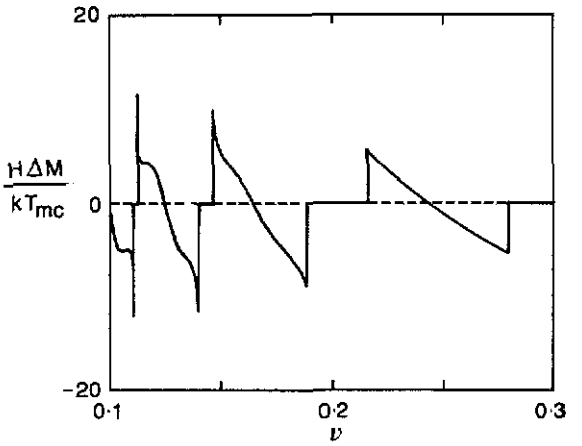

Figure 6. The magnetization change ΔM along the melting curve, expressed as $H\Delta M/kT_{mc}$, for comparison with the magnetization deduced thermodynamically (Lea *et al* 1991).

energy gaps Δ_ν. Ordered states at other fractional values of ν may also produce cusps in ΔE, but the energy gaps may well be smaller. Only if $\Delta E = E_L - E_S < 0$ will a re-entrant phase occur.

The phase boundary for $T > 0$ can, in principle, be found by equating the free energies $F_S = F_L$ and hence

$$T_m = (E_L - E_S)/(S_L - S_S) = \Delta E/\Delta S \tag{13}$$

where ΔE and ΔS are evaluated along the melting curve. For the purposes of this discussion we will assume that the entropy of the solid is small compared with the liquid and hence that $\Delta S \simeq S_L$, the entropy of the liquid. If $\Delta E > 0$, but S_L decreases near a fractional state, then T_m would increase rapidly and the neglect of the solid entropy would no longer be a good approximation. Indeed if the solid entropy becomes greater than S_L while $\Delta E > 0$, an increase in temperature will stabilize the solid phase. However, along the melting curve, which is the region of interest here, thermal excitations will probably smooth out the variations in S_L shown in figure 4, and also any small cusps in ΔE. To demonstrate the origin of the observed melting curve, we have therefore used the internal energy shown in figure 5, and an entropy variation that asymptotically approaches the calculated entropy, equation (10), for values of ν close to the liquid ground states. We have taken the energy gaps to increase with ν as $\Delta_\nu = 0.054\nu$. The resultant phase diagram, as calculated from (13) is shown in figure 1(*b*) for $\nu > 0.1$. This does indeed have some of the features of the melting curve postulated from the experimental results, although further structure may also occur in the phase diagram at other ordered states.

We can also assume that the magnetization difference between the two phases is dominated by the field-dependent magnetization discussed above and that $\Delta M \simeq M_L$, the magnetization of the liquid phase. Introducing $t_m = T_m/T_{mc}$ we can then write (2) as

$$\partial t_m/\partial\nu = \pm\sqrt{2}\Gamma_m\Delta_\nu/\nu^{3/2}S(\nu) \tag{14}$$

close to the liquid ground state. Note the important property that $\partial t_m/\partial \nu$ is a function only of ν, as required by scaling arguments (Tao 1990). All the thermodynamic functions should depend only on ν and $t = T/T_{mc}$ in this region of the (t, ν) plane. The magnetization change along the melting curve $\Delta M = -(\partial \Delta F/\partial H)_T$ as calculated from our simple model is shown in figure 6 and shows the features that were derived from thermodynamic arguments by Lea *et al* (1991).

5. Discussion and summary

In summary we have

(i) proposed a phenomenological model for which the analogue, equation (1), of the Clausius–Clapeyron equation for the melting curve of a Wigner crystal can be integrated—the simplest model of the phase boundaries of the phases C_2–C_4 in figure 1 gives a re-entrant phase diagram;

(ii) calculated the magnetization of two closely related microscopic models: (a) an anyon gas model in the classical limit and (b) a composite fermion model, which complements (a) in that the magnetization and entropy are determined at low temperatures.

While the present models do not allow a fully quantitative prediction of the melting curve of the two-dimensional Wigner crystal, the main features of the magnetization of the electron liquid are reproduced by the two microscopic models (a) and (b) above. It is our distinct impression that the present work supports the usefulness of the anyon concept in magnetic fields, although further work remains to be done to relate the model to the composite fermion approach. Currently, our view is that the two models are complementary—one being readily calculable in the classical limit and the other being most tractable at low temperatures. Both models, in the end, relate to an electron associated with an integral number of flux lines, and the decomposition into 'fermions plus additional flux lines', as opposed to 'anyons' may be a matter of semantics, although we have at present no decisive conclusion on this point†. Our final comment is that while we feel that our work supports the model for anyons in magnetic fields, no conclusions are to be drawn from the present study as to the usefulness, or otherwise, of the model of field-free anyons in the context of high-temperature superconductivity.

Acknowledgments

This collaboration began during a visit by one of us (WS) to the Theoretical Chemistry Department, University of Oxford, and we gratefully acknowledge support from the Pohang Institute of Science and Technology and the Ministry of Education in Korea.

References

Andrei E Y, Deville G, Glattli D C, Williams F I B, Paris E and Etienne B 1988 *Phys. Rev. Lett.* **60** 2765

† Since this work was completed, the work of Cho and Rim (1992 *Ann. Phys.* **213** 295) has appeared and is relevant to dealing with Bose–Einstein condensation anyons.

Buhmann H, Joss W, von Klitzing K, Kukuskin I V, Plaut A S, Martinez G, Ploog K and Timofeev V B 1991 *Phys. Rev. Lett.* **66** 926
Deville G 1988 *J. Low Temp. Phys.* **72** 135
Dowker J S and Chang M 1990 *ICTP Report* ICTP, Trieste
Durkan J, Elliott R J and March N H 1968 *Rev. Mod. Phys.* **40** 812
Glattli D C, Andrei E Y, Clarke R S, Deville S, Dorin C, Etienne B E, Foxon C T, Harris J J, Paris E, Probst O, Williams F I B and Wright P A 1991 *Physica* B **169** 328
Isihara A 1989 *Solid State Physics* vol 42 (New York: Academic) p 272
Jain J K 1989 *Phys. Rev. Lett.* **63** 199
—— 1990 *Phys. Rev.* B **41** 7653
—— 1992 *Proc. 9th Int. Conf. on Electronic Properties of Two-Dimensional Systems: Surf. Sci.* **263** at press
Jain J K and Goldman V J 1992 *Phys. Rev.* B **45** 1255
Johnson M D and Canright G S 1990 *Phys. Rev.* B **41** 6870
Lea M J, March N H and Sung W J 1991 *J. Phys.: Condens. Matter* **3** 4301
Lee D-H 1991 *Physica* B **169** 37
Li Y P, Sajoto T, Engel L W, Tsui D S and Shagegan M 1991 *Phys. Rev. Lett.* **67** 1630
Plaut A S, Buhmann H, Joss W, von Klitzing K, Kukuskin I V, Martinez G, Ploog K and Timofeev V B 1991 *Physica* B **169** 557
Tao Z C 1990 *Phys. Lett.* A **151** 172
Wilczek F 1990 *Anyons* (Singapore: World Scientific)